



A novel precursor in preparation and characterization of nickel oxide nanoparticles via thermal decomposition approach

Masoud Salavati-Niasari^{a,b,*}, Noshin Mir^b, Fatemeh Davar^a

^a Institute of Nano Science and Nano Technology, University of Kashan, Kashan, P.O. Box 87317-51167, Islamic Republic of Iran

^b Department of Inorganic Chemistry, Faculty of Chemistry, University of Kashan, Kashan, P.O. Box. 87317-51167, Islamic Republic of Iran

ARTICLE INFO

Article history:

Received 24 August 2009

Received in revised form

22 November 2009

Accepted 23 November 2009

Available online 26 November 2009

Keywords:

Nanostructured materials

Chemical synthesis

ABSTRACT

In order to raise the need of co-surfactant in the synthesis of NiO nanoparticles, [bis(2-hydroxy-1-naphthaldehydato)nickel(II)] complex was employed as a novel precursor in thermal decomposition process using oleylamine (C₁₈H₃₇N) as surfactant. The products were characterized by X-ray diffraction (XRD), scanning electron microscopy (SEM), transmission electron microscopy (TEM), Fourier transform infrared (FT-IR) spectroscopy, thermogravimetric analysis (TGA), X-ray photoelectron spectroscopy (XPS) and ultraviolet–visible (UV–Vis) spectroscopy. Also the novel precursor thermally was treated in solid state reaction in different temperature, 400, 500, and 600 °C. Synthesized nickel oxide nanoparticles have a cubic phase with average size of 15–20 nm.

© 2009 Elsevier B.V. All rights reserved.

1. Introduction

Nanostructured materials have attracted great interest in both fundamental as well as applied research areas due to their outstanding physical and chemical properties and also promising applications in nanodevices [1]. A reduction in particle size to nanometer scale results in various interesting properties compared to their bulk properties. Nickel oxide (NiO) is a material that has been the subject of a considerable number of research studies, mostly on the basis of the unique electrical, optical and magnetic properties of the material [2]. NiO is considered a prototypical p-type, wide band gap (3.6–4.0 eV) semiconductor [3,4]. The electronic properties of NiO have specifically driven research interests in applications such as anodes for lithium ion batteries [5], solar cells [6], electrochromic coatings [7], composite anodes for fuel cells [8,9], antiferromagnetic materials [10] and in chemical (gas) sensing [11]. Furthermore, nickel oxides are being studied for applications in smart windows, electrochemical supercapacitors [12] and dye-sensitized photocathodes [13].

In accomplishing manipulation of the nanostructured nickel oxide, a variety of strategies have been employed, such as evaporation [14], sputtering [15], electrodeposition [16], thermal decomposition [17] and sol-gel techniques [18]. Thermal decomposition method has some advantages such as simple process,

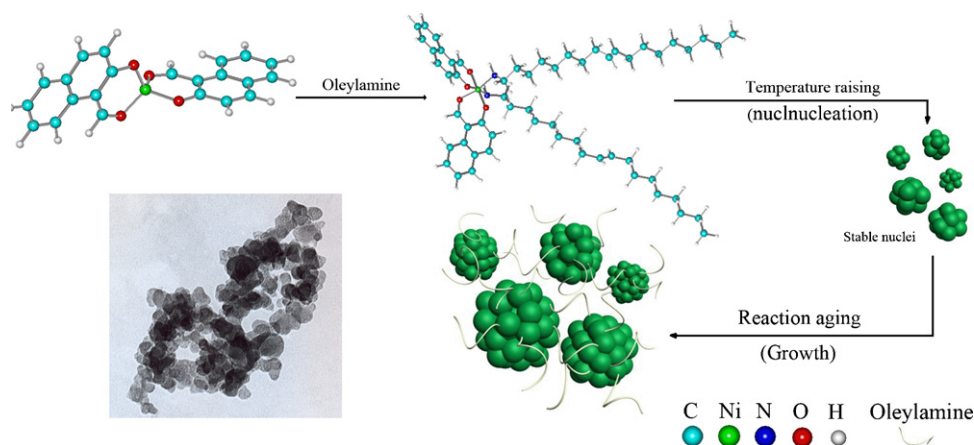
low-cost and easiness to obtain high purity products hence it is quite promising and facile rout for industrial applications.

To exploit the size-dependent properties materials exhibit, it is important to be able to prepare nanomaterials with a controlled size and size distribution. In this regard, utilization of a natural surfactant is an interesting possibility in the synthesis of nanoparticles [19,20] due to its many advantages such as biodegradability and lower toxicity [21]. By controlling the growth of the particles, surfactants play an important role in synthetic procedure and lead to nanoparticles with controlled size and a narrow size distribution. In addition of the important role of surfactants in size control of nanoparticles, precursors with special structures and shapes also can prevent of agglomeration. The concept of co-assembling inorganic precursor molecules with amphiphile organic molecules for controlling the structure and organization of inorganic materials has successfully been used to produce materials with both scientific and technological importance. At the moment a major interest is in the development of organometallic or inorganic precursors [22,23]. Recently Zeng and Zhang have used 6-coordinated nickel ion complex [Ni(EDA)₃]²⁺ and reported the Hollow and core-shell β-Ni(OH)₂ nanospheres [24]. Very recently our group has reported the synthesis of nickel oxide (NiO) nanoclusters via thermal decomposition of nickel oxalate [25].

In the continuation of previous works we decided to prepare NiO nanocrystals from [bis(2-hydroxy-1-naphthaldehydato)nickel(II)] complex; [Ni(HNA)₂]; as a new precursor. To the best of our knowledge the use of [Ni(HNA)₂] as precursor in nanoparticles synthesis approach is the first time. Here, we report a simple, green, low-cost, and reproducible process for the synthesis of NiO nanocrystals.

* Corresponding author at: Institute of Nano Science and Nano Technology, University of Kashan, Kashan, P.O. Box 87317-51167, Islamic Republic of Iran. Tel.: +98 361 5555333; fax: +98 361 5552935.

E-mail address: salavati@kashanu.ac.ir (M. Salavati-Niasari).



Scheme 1. Schematic diagram illustrating the formation of NiO nanoparticles (sample 1).

In this process, oleylamine was used as both the medium and the stabilizing reagent.

2. Experimental

2.1. Materials

All the chemical reagents used in our experiments were of analytical grade and were used as received without further purification. Oleylamine, toluene, hexane, and ethanol were purchased from Aldrich and used as received. The precursor complex; $[\text{Ni}(\text{HNA})_2]$ was prepared according to this procedure: the $\text{Ni}(\text{OOCCH}_3)_2 \cdot \text{H}_2\text{O}$ (2 mmol) was dissolved into 10 mL of methanol to form a homogeneous solution. A stoichiometric amount of 2-hydroxy-1-naphthaldehyde dissolved in an equal volume of methanol was dropwise added into the above solution under magnetic stirring. The solution was refluxed in 60°C for about 2 h and a green precipitate was centrifuged and washed with ethanol several times. The product was dried at 70°C . The [bis(2-hydroxy-1-naphthaldehydato)nickel(II)] complex was characterized by FT-IR, elemental analyses, and thermo gravimetric analysis (TGA). Anal. Calcd. for $[\text{Ni}(\text{HNA})_2]$: C, 65.87; H, 3.50, Ni, 14.69. Found: C, 65.92; H, 3.55; Ni, 14.76%. IR (FT-IR method): 2920 (CH_3), 2854 (CH_2), 1590 (CO), 1470–1415 (CH_3 , CH_2) cm^{-1} .

2.2. Characterization

X-ray diffraction (XRD) patterns were recorded by a Rigaku D-max C III, X-ray diffractometer using Ni-filtered $\text{Cu K}\alpha$ radiation. Elemental analyses were obtained from Carlo ERBA Model EA 1108 analyzer. Scanning electron microscopy (SEM) images were obtained on Philips XL-30ESEM. Transmission electron microscopy (TEM) image was obtained on a Philips EM208 transmission electron microscope with an accelerating voltage of 100 kV. Fourier transform infrared (FT-IR) spectra were recorded on Shimadzu Varian 4300 spectrophotometer in KBr pellets. The electronic spectra of the complexes were taken on a Shimadzu Ultraviolet–visible (UV–vis) scanning spectrometer (Model 2101 PC). Thermogravimetric-differential thermal analysis (TG-DTA) were carried out using a thermal gravimetric analysis instrument (Shimadzu TGA-50H) with a flow rate of 20.0 mL min^{-1} and a heating rate of $10^\circ\text{C min}^{-1}$ under N_2 atmosphere. X-ray photoelectron spectroscopy (XPS) of the as-prepared products was measured on an ESCA-3000 electron spectrometer with nonmonochromatized $\text{Mg K}\alpha$ X-ray as the excitation source.

2.3. Synthesis of NiO nanoparticles (sample 1)

The main synthetic procedure in order to approach to final products is a modified version of the method developed by Hyeon and others for the synthesis of metal nanocrystals that employ the thermal decomposition of transition metal complexes [26,27]. In this synthesis, NiO nanoparticles (sample 1) were prepared by the thermal decomposition of $[\text{Ni}(\text{HNA})_2]$ -oleylamine complex as precursor. The $[\text{Ni}(\text{HNA})_2]$ -oleylamine complex was prepared by reaction 0.5 g of $[\text{Ni}(\text{HNA})_2]$ with 5 mL of oleylamine. The mixed solution was placed in a 25 mL flask and heated up to 145°C for 60 min. At this moment, the temperature was increased to 245°C . The solution was aged at 245°C for 60 min, and was then cooled to room temperature. The black nanoparticles were precipitated by adding 15 mL ethanol to the solution. The final products were washed with ethanol for at least three times to remove impurities, if any, and dried at 100°C . This product could easily be re-dispersed in nonpolar organic solvents, such as hexane or toluene (Scheme 1). The synthesized nanoparticles were characterized by XRD, SEM, TEM, FT-IR, XPS and UV–vis techniques.

3. Results and discussion

The thermal observation of the as-prepared precursor was investigated with thermal gravimetric analysis (TGA). Fig. 1 shows that $[\text{Ni}(\text{HNA})_2]$ start to decompose at 180°C and the weight loss happens in the temperature range 180 – 300°C . The weight loss may be ascribed to the decomposition of the $[\text{Ni}(\text{HNA})_2]$. The weight loss is about 81.20%, which is close to the theoretical value (81.38%). Based on the TGA results, the main weight loss has occurred at 300°C , so we should thermally decompose the precursor at this point, however using capping ligands like $\text{C}_{18}\text{H}_{37}\text{N}$ caused precursor to be decomposed at lower temperature.

The XRD diffraction pattern of the sample 1 was recorded for the identification of the product (Fig. 2). The main diffraction peaks were observed at 37.80° , 43.45° , 62.82° , 75.20° and 79.90° . The XRD pattern of the sample 1 confirms that the formed material is nickel oxide. All diffraction peaks can be indexed to the pure NiO crystalline phase (space group: $Fm\bar{3}m$). The crystallite size diameter (D) of the NiO nanoparticles has been calculated by Debye–Scherrer equation:

$$D = \frac{0.9\lambda}{\beta \cos \theta}$$

where β -FWHM (full-width at half-maximum, or half-width) is in radians and θ is the position of the maximum of diffraction peak and λ is the X-ray wavelength (1.5406 \AA for $\text{Cu K}\alpha$). Crystallite size of initial powder has been found to be $17 \pm 1 \text{ nm}$.

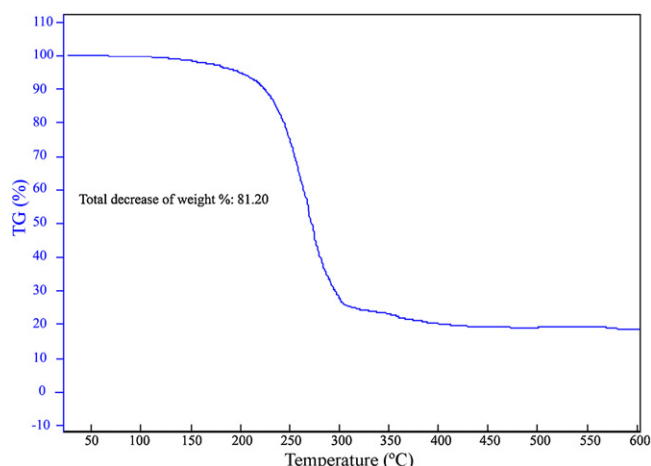


Fig. 1. TGA of the $[\text{Ni}(\text{HNA})_2]$ precursor.

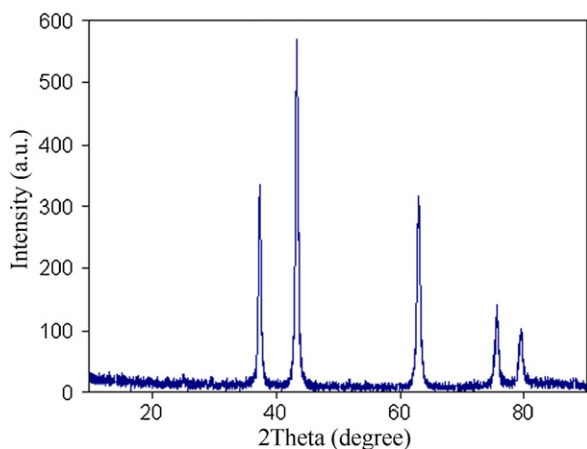


Fig. 2. XRD pattern of the NiO nanoparticles.

Investigating capping of organic surfactants on the surface of nanoparticles, the Fourier transformed infrared (FT-IR) of the as-synthesized samples was performed. Fig. 3 shows a comparison of FT-IR spectrum of (a) $[\text{Ni}(\text{HNA})_2]$, (b) NiO nanoparticles, and (c) oleylamine. The broad peaks at ca. $3350\text{--}3400\text{ cm}^{-1}$ in Fig. 3a and b are due to adsorbed water on the external surface of the samples during handling to record the spectra. The H-OH bending vibration appears at 1635 cm^{-1} . In our measurement, number of weak peaks between $\nu 1000\text{--}1400\text{ cm}^{-1}$ and $\nu 2800\text{--}3000\text{ cm}^{-1}$ are attributable to the symmetric and asymmetric stretching of the $-\text{CH}_2$ groups, terminal $-\text{CH}_3$ and $=\text{CH}$ of $\text{C}_{18}\text{H}_{37}\text{N}$ and corresponds with oleylamine spectra (Fig. 3c). Also a characteristic broad band due to the C-N stretching mode was present at about 1170 cm^{-1} . So the oleylamine serves as the capping ligand that controls growth [27]. Finally, the peak at 455 cm^{-1} in spectrum (Fig. 3b), showing Ni-O bonds, gave clear evidence about the presence of the NiO.

The surface morphological study of the NiO nanoparticles was carried out using SEM image. Fig. 4a shows the SEM image of the NiO (sample 1). It is seen that the products are tiny, aggregated nanoparticles with spherical shapes. TEM photograph of the product has been given in Fig. 4b. The size of nanoparticles obtained from the XRD diffraction patterns are in close agreement with the TEM

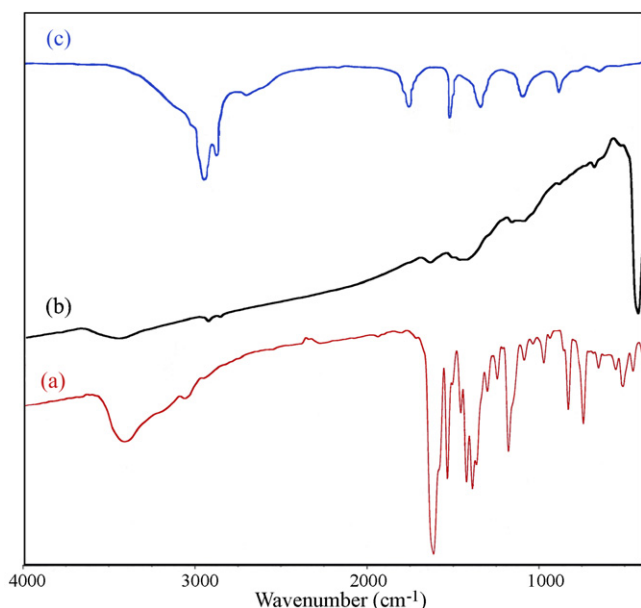


Fig. 3. FT-IR spectra of (a) $[\text{Ni}(\text{HNA})_2]$, (b) NiO nanoparticles, and (c) free oleylamine.

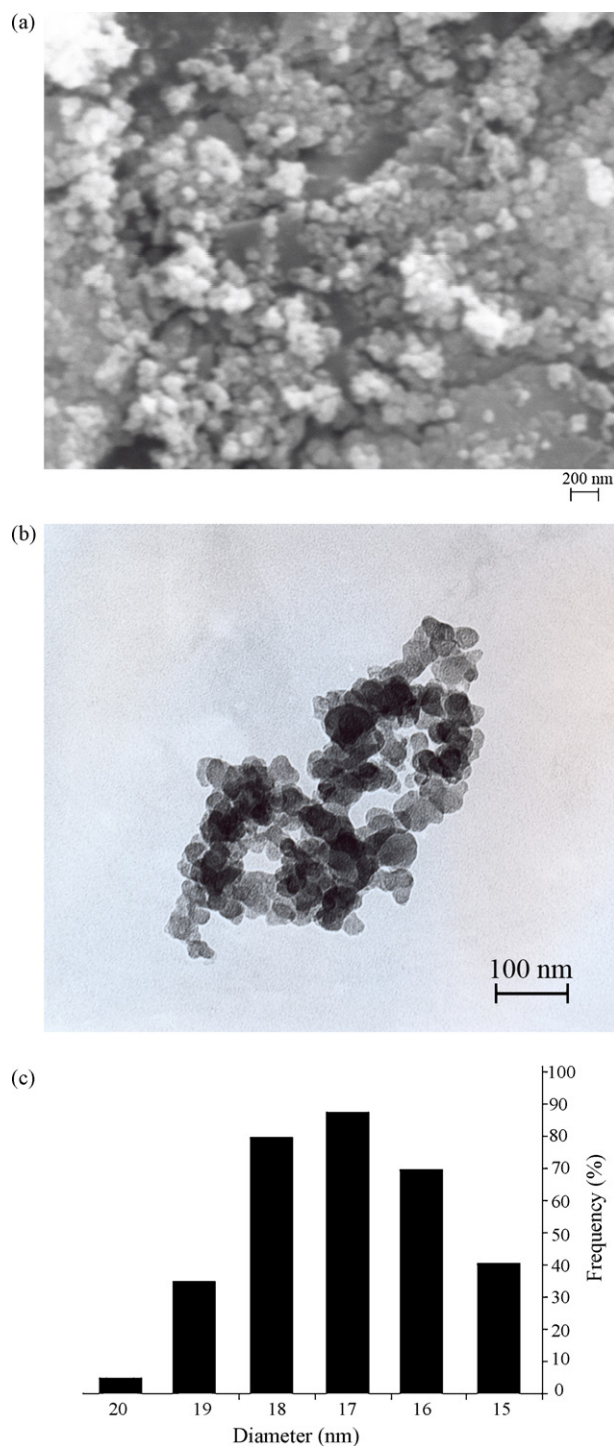


Fig. 4. (a) SEM, (b) TEM images and (c) size distribution histogram of NiO nanoparticles.

studies which show sizes of 15–20 nm. These particles are nearly spherical and confirm the SEM micrograph. It is observed that in spite of agglomeration of nanoparticles, they have a narrow size distribution. To investigate the size distribution of the nanoparticles a particle size histogram was prepared for sample 1 (Fig. 4c). This size distribution is centered at a value of 17 nm.

Fig. 5 is the UV-Vis spectrum of the as-synthesized NiO nanoparticles dispersed in ethanol. A strong absorption in the UV region is observed at wavelengths about 323 nm. The strong absorption in the UV region is attributed to band gap absorption in NiO [28]. It

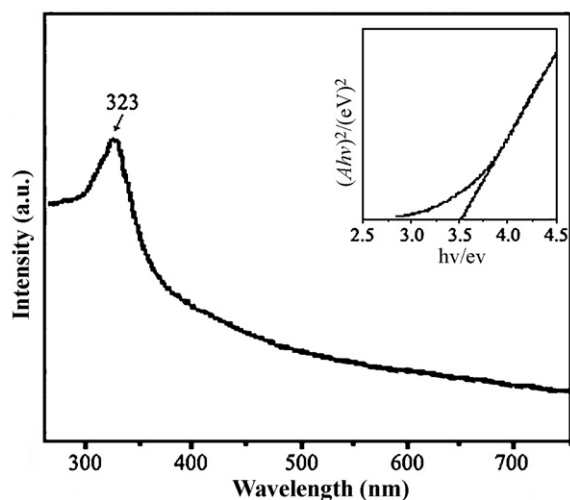


Fig. 5. UV-vis absorption spectrum of the NiO nanoparticles dispersed in ethanol.

is well known that optical band gap (E_g) can be calculated on the basis of the optical absorption spectrum by the following equation:

$$(Ah\nu)^n = B(h\nu - E_g)$$

where $h\nu$ is the photo energy, A is absorbance, B is a constant relative to the material and n is either two for direct transition or $1/2$ for an indirect transition [29]. Hence, the optical band gap for the absorption peak can be obtained by extrapolating the linear portion of the $(Ah\nu)^n - h\nu$ curve to zero. The band gap of the NiO particles is about 3.52 eV, which is similar to the value (3.55 eV) reported by Boschloo and Hagfeldt [30]. No linear relation was found for $n = 1/2$, suggesting that the as-prepared NiO nanoparticles are semiconducting with direct transition at this energy [28].

Further evidence for the chemical state and the purity and the composition of the products was obtained by X-ray photoelectron spectra (XPS). Fig. 6 shows the XPS pattern of the as-prepared sample 1 (NiO nanoparticles). The XPS spectra of NiO nanoparticles show two main peaks of $2p_{3/2}$ and $2p_{1/2}$ at 856.1 and 874.1 eV, which can be assigned to the Ni(II) ion in the NiO particles. In turn, the binding energy of Ni $2p_{3/2}$ peak was shifted around 2.0 eV to higher values compared to that of pure NiO (854.4 eV) with higher proportions of Ni(II) ions in the oxide form than in the spinel form [31]. The main reason for this shift is due to the oxygen vacancy existing on the surface. The following results would prove this speculation. Tomellini attributed this peak to Ni^{3+} species on the NiO surface [32]. Other researcher reported that the intensity of this peak increased with the concentration of the defects [33]. The O 1s peak at 530.7 eV is attributed to the (O^{2-}) in the NiO. The binding energies of the main and satellite peaks in the O 1s and Ni 2p core levels are consistent with the previous report on NiO [34].

The spectroscopy results of as-synthesized NiO nanoparticles (sample 1) suggest a three-step mechanism for the nanoparticles growth. Turkevich who established the first reproducible standard procedure for the preparation of metal colloids, also proposed a mechanism for the stepwise formation of nanoparticles based on nucleation, growth, and agglomeration [35]. In this work, in the presence of oleylamine as solvent, $[Ni(HNA)_2]$ -oleylamine is synthesized. After raising the temperature, $[Ni(HNA)_2]$ -oleylamine decomposes, initiate nucleation occur and stable nuclei are formed. To initiate nucleation, the concentration of metal atoms in solution must be high enough to reach "supersaturation" [36]. To achieve a monodisperse sample, the nucleation event must be complete before the growth step begins. A further critical issue for gaining high-quality nanoparticles is the passivation of the metallic surface

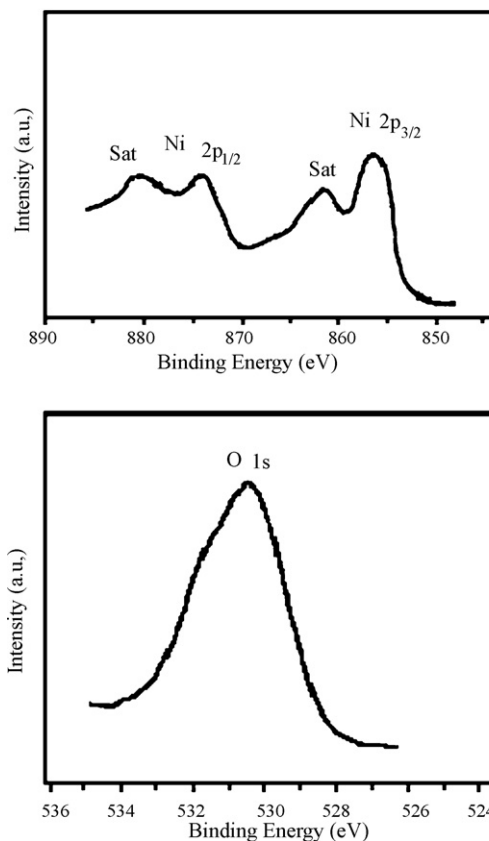


Fig. 6. XPS spectrum of NiO nanoparticles.

by adding organic molecules. Surface passivation helps to achieve size selectivity, prevent agglomeration and fusing of particles, and provide for the solubility of the particles in the desired organic or aqueous medium [37]. Oleylamine is known as a ligand that binds tightly to the metal nanoparticles surface and in this reaction it is both as solvent and capping agent. The long carbon chain of oleylamine can provide great steric hindrance to control the size of metal nanoparticles. On this step, oleylamine passivates the surface of grown nanoparticles and prevent agglomeration. The presence of oxygen in the reaction flask is the reason of NiO nanoparticles production instead of metallic Ni nanoparticles. The growth of the NiO nanocrystals with spherical shapes can be explained on the basis of the schematic view presented in Scheme 1.

The choice of metal precursor is a key step in the preparation of nanometal oxides [38–42]. Many different precursors have been used for simple preparation of these nanoparticles [43–45]. The priority of using $[Ni(HNA)_2]$ complex as a novel precursor is its great steric hindrance which raise the need of using a co-surfactant beside the main surfactant. In Table 1 some of the precursors used in thermal decomposition process are compared with the present work. According to these results, by thermal decomposition of $[Ni(HNA)_2]$ complex, NiO nanoparticles were synthesized successfully with the best conditions and smallest size.

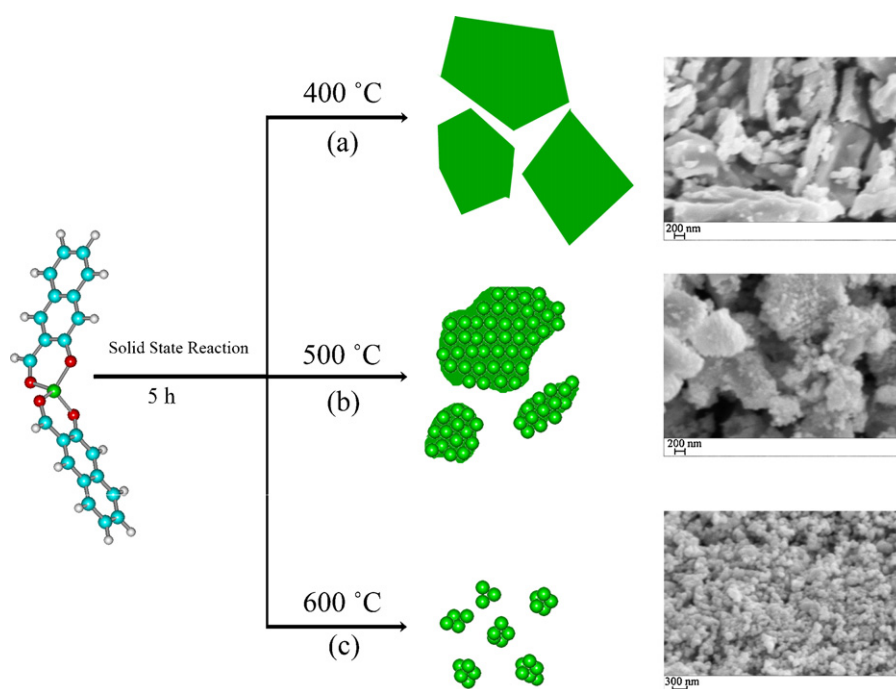
In addition, some other conditions were examined to investigate the morphology of products, if any, and compare them with each other. According to Table 2 two different approaches including thermal processes in presence and in absence of capping agents were examined. In the first approach, samples 1 and 2 were investigated in presence of protecting agent which the former was discussed before. In condition of using both oleylamine and triphenylphosphine (TPP) as capping agent (sample 2), after washing with organic solvents no products were observed. Since in presence

Table 1
Comparison of particle size of NiO by thermal decomposition method in several works.

Sample	Precursor	Surfactant	Co-surfactant	T (°C)	Reaction time (h)	Particle size (nm) (according to XRD results)
1	Ni ₃ (NO ₃) ₂ (OH) ₄ [43]	–	–	400	4	54
2	Nickel dimethylglyoximate [45]	–	–	500	2	35
3	Ni(OAc) ₂ [28]	Polyvinylpyrrolidone (PVP)	–	400	2	30
4	Nickel oxalate [45]	Cetyltrimethylammonium bromide (CTAB)	n-Butanol	450	6	30
5	[Ni(HNA) ₂] (present work)	Oleylamine	–	245	1	15

Table 2
Two different approaches for synthesis of NiO nanoparticles.

Sample	Capping agent	T (°C)	Time (min)	Composition of the products and particle size (nm) (according to XRD results)
1	Oleylamine	245	60	NiO nanoparticles, 15–20 nm
2	Oleylamine + TPP	245	60	No product
3	–	400	300	[Ni(HNA) ₂] (main) + NiO (minor)
4	–	500	300	NiO (main) + [Ni(HNA) ₂] (minor) agglomerated nanoparticles
5	–	600	300	NiO nanoparticles



Scheme 2. Schematic diagram illustrating the solid state reaction of precursor in (a) 400 °C, (b) 500 °C, and (c) 600 °C.

of other precursors using the combination of oleylamine and TPP resulted in good product with a narrow size distribution [25], it is suggested that because of the ring steric hindrance of the precursor, TPP which contains large chunks cannot cap on the NiO particles (sample 2) and this hindrance prevents oleylamine approach to the metallic center. Therefore, it is deduced that steric hindrance of the novel precursor acts like a protecting agent and there is no need to apply two capping agents simultaneously anymore [26]. To investigate the importance of surfactant role in temperature decrease, in the second approach [Ni(HNA)₂] were calcined at 400, 500 and 600 °C for 5 h without using any surfactant (samples 3–5, respectively). A schematic view of second approach and morphology of the products are shown by SEM images in Scheme 2. It is clear that 400 °C is not the required temperature for decomposition of precursor and no nanoparticle is formed (Scheme 2a). As the temperature is increased, agglomerated nanoparticles form at 500 °C (Scheme 2b) and they get separated at 600 °C (Scheme 2c). Considering different conditions employed to prepare these sam-

ples, it is obvious that using oleylamine as capping agent decreases the reaction temperature and is preferred for NiO nanoparticles synthesis.

4. Conclusion

NiO nanoparticles have been successfully synthesized through a thermal decomposition of new precursor [Ni(HNA)₂] in the presence of C₁₈H₃₇N. This precursor has steric hindrance and therefore there was no need to use two surfactants for size control. Also the novel precursor was thermally treated without using any surfactant and the results showed that surfactant has an important role in decrease of reaction temperature. From the results of XRD, FT-IR and TEM, the obtained NiO nanoparticles *via* decomposition of precursor in the presence of oleylamine at 245 °C for 60 min, show good morphologies corresponding to nanosize about 15–20 nm, relatively.

Acknowledgements

Authors are grateful to the Council of University of Kashan for their unending effort to provide financial support to undertake this work.

References

- [1] D.-B. Kuang, B.-X. Lei, Y.-P. Pan, X.-Y. Yu, C.-Y. Su, *J. Phys. Chem. C* 113 (2009) 5508–5513.
- [2] E.R. Beach, K.R. Shqau, S.E. Brown, S.J. Rozeveld, P.A. Morris, *Mater. Chem. Phys.* 115 (2009) 371–377.
- [3] H.-L. Chen, Y.-M. Lu, W.-S. Hwang, *Surf. Coat. Technol.* 198 (2005) 138–142.
- [4] H. Sato, T. Minami, S. Takata, T. Yamada, *Thin Solid Films* 236 (1993) 27–31.
- [5] H.K. Liu, G.X. Wang, Z.P. Guo, J.Z. Wang, K. Konstantinov, *T. Jour. New Mater. Electrochem. Syst.* 10 (2007) 101–104.
- [6] J. Bandara, H. Weerasinghe, *Solar Energy Mater. Solar Cells* 85 (2005) 385–390.
- [7] C.G. Granqvist, G.A. Niklasson, A. Azens, *Appl. Phys. A: Mater. Sci. Proc.* 89 (2007) 29–35.
- [8] J.G. Cheng, L.P. Deng, B.R. Zhang, P. Shi, G.Y. Meng, *Rare Met.* 26 (2007) 110–117.
- [9] V. Esposito, D.Z. de Florio, F.C. Fonseca, E.N.S. Muccillo, R. Muccillo, E. Traversa, *J. Eur. Ceram. Soc.* 25 (2005) 2637–2641.
- [10] M. Ghosh, K. Biswas, A. Sundaresan, C.N.R. Rao, *J. Mater. Chem.* 16 (2006) 106–111.
- [11] C.Y. Lee, C.M. Chiang, Y.H. Wang, R.H. Ma, *Sens. Actuators B: Chem.* 122 (2007) 503–510.
- [12] V. Srinivasan, J. Weidner, *J. Electrochem. Soc.* 144 (1997) L210–L213.
- [13] J. He, H. Lindström, A. Hagfeldt, S.E. Lindquist, *J. Phys. Chem. B* 103 (1999) 8940–8943.
- [14] R. Cinnsealach, G. Boschloo, S.N. Rao, D. Fitzmaurice, *Solar Energy Mater. Solar Cells* 57 (1999) 107–125.
- [15] K. Yoshimura, T. Miki, S. Tanemura, *Jpn. J. Appl. Phys.* 34 (1995) 2440–2446.
- [16] C. Natarajan, H. Matsumoto, G. Nogami, *J. Electrochem. Soc.* 144 (1997) 121–126.
- [17] C.S. Carney, C.J. Gump, A.W. Weimer, *Mater. Sci. Eng. A* 431 (2006) 1–12.
- [18] A. Surca, B. Orel, B. Pihlar, P. Bukovec, *J. Electroanal. Chem.* 408 (1996) 83–100.
- [19] H. Kamiya, K. Gomi, Y. Iida, K. Tanaka, T. Yoshiyasu, T. Kakiuchi, *J. Am. Ceram. Soc.* 86 (2003) 2011–2018.
- [20] R.H. Becerra, C. Zorrilla, J.L. Rius, J.A. Ascencio, *Appl. Phys. A* 91 (2008) 241–246.
- [21] P. Palanisamy, A.M. Raichur, *Mater. Sci. Eng. C* 29 (2009) 199–204.
- [22] M. Salavati-Niasari, N. Mir, F. Davar, *J. Alloys Compd.* 476 (2009) 908–912.
- [23] M. Salavati-Niasari, F. Davar, M. Mazaheri, *J. Alloys Compd.* 47 (2009) 502–506.
- [24] S. Zhang, H.C. Zeng, *Chem. Mater.* 21 (2009) 871–883.
- [25] M. Salavati-Niasari, N. Mir, F. Davar, *Polyhedron* 28 (2009) 1111–1114.
- [26] J. Park, E. Kang, S.U. Son, H.M. Park, M.K. Lee, J. Kim, K.W. Kim, H.-J. Noh, J.-H. Park, C.J. Bae, J.-G. Park, T. Hyeon, *Adv. Mater.* 17 (2005) 429–434.
- [27] M. Salavati-Niasari, F. Davar, M. Mazaheri, M. Shaterian, *J. Magn. Magn. Mater.* 320 (2008) 575–578.
- [28] X. Li, X. Zhang, Z. Li, Y. Qian, *Solid State Commun.* 137 (2006) 581–584.
- [29] A. Hagfeldt, M. Gratzel, *Chem. Rev.* 95 (1995) 49–68.
- [30] G. Boschloo, A. Hagfeldt, *J. Phys. Chem. B* 105 (2001) 3039–3044.
- [31] Y. Hattori, T. Konishi, K. Kaneko, *Chem. Phys. Lett.* 355 (2002) 37–42.
- [32] M.J. Tomellini, *J. Electron Spectrosc. Relat. Phenom.* 58 (1992) 75–78.
- [33] B. Zhao, X.-K. Ke, J.-H. Bao, C.-L. Wang, L. Dong, Y.-W. Chen, H.-L. Chen, *J. Phys. Chem. C* 113 (2009) 14440–14447.
- [34] B. Varghese, M.V. Reddy, Z. Yanwu, C.S. Lit, T.C. Hoong, G.V.S. Rao, B.V.R. Chowdari, A.T.S. Wee, C.T. Lim, C.-H. Sow, *Chem. Mater.* 20 (2008) 3360–3367.
- [35] J. Turkevich, *Gold Bull.* 18 (1985) 86–91.
- [36] C.B. Murray, C.R. Kagan, M.G. Bawendi, *Annu. Rev. Mater. Sci.* 30 (2000) 545–610.
- [37] B. Corain, G. Schmid, N. Toshima (Eds.), *Metal Nanoclusters in Catalysis and Materials Science: The Issue of Size Control*, Elsevier Publishers, Oxford, 2008, pp. 21–23.
- [38] M. Salavati-Niasari, F. Davar, *Mater. Lett.* 63 (2009) 441–443.
- [39] F. Davar, Z. Fereshteh, M. Salavati-Niasari, *J. Alloys Compd.* 476 (2009) 797–801.
- [40] A. Ahniyaz, G.A. Seisenbaeva, L. Häggström, S. Kamali, V.G. Kessler, P. Nordblad, C. Johansson, L. Bergström, *J. Magn. Magn. Mater.* 320 (2008) 781–787.
- [41] S. Baskoutas, P. Giabouranis, S.N. Yannopoulos, V. Dracopoulos, L. Toth, A. Christanthopoulos, N. Bouropoulos, *Thin Solid Films* 515 (2007) 8461–8464.
- [42] M. Salavati-Niasari, F. Davar, M. Mazaheri, *Mater. Lett.* 62 (2008) 1890–1892.
- [43] J. Estellé, P. Salagre, Y. Cesteros, M. Serra, F. Medina, J.E. Sueiras, *Solid State Ionics* 156 (2003) 233–243.
- [44] D. Tao, F. Wei, *Mater. Lett.* 58 (2004) 3226–3228.
- [45] T. Ahmad, K.V. Ramanujachary, S.E. Lofland, A.K. Ganguli, *Solid State Sci.* 8 (2006) 425–430.